

Novel, Highly Potent Aldose Reductase Inhibitors: Cyano(2-oxo-2,3-dihydroindol-3-yl)acetic Acid Derivatives

Federico Da Settimo,^{*,§} Giampaolo Primofiore,[§] Antonio Da Settimo,[§] Concettina La Motta,[§] Francesca Simorini,[§] Ettore Novellino,[‡] Giovanni Greco,[‡] Antonio Lavecchia,[‡] and Enrico Boldrini[†]

Dipartimento di Scienze Farmaceutiche, Università di Pisa, Via Bonanno 6, 56126 Pisa, Italy, Dipartimento di Chimica Farmaceutica e Tossicologica, Università di Napoli "Federico II", Via Domenico Montesano, 49, 80131 Napoli, Italy, and Farmigea S.p.A., Via Carmignani 2, 56127, Pisa, Italy

Received January 10, 2003

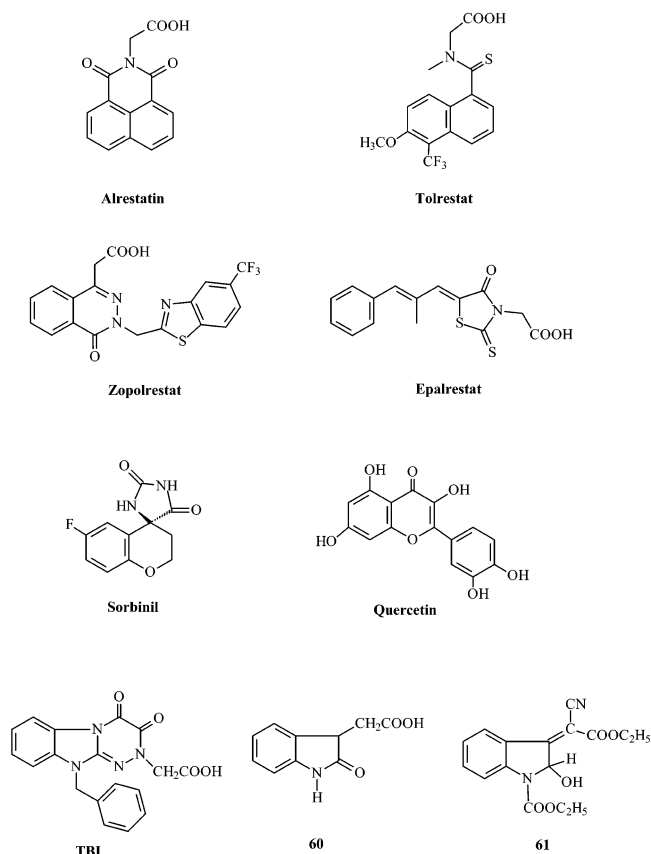
Cyano(2-oxo-2,3-dihydroindol-3-yl)acetic acid derivatives were synthesized and tested as a novel class of aldose reductase (ALR2) inhibitors. Each compound was evaluated as a diastereomeric mixture, due to tautomeric equilibria in solution. The parent compound **39** exhibited a good inhibitory activity with an IC_{50} value of $0.85 \mu\text{M}$, similar to that of the well-known ARI sorbinil (IC_{50} $0.50 \mu\text{M}$). The concurrent introduction of a halogen and a lipophilic group in the 5- and in the 1-positions, respectively, of the indole nucleus of **39**, gave compound **55**, cyano[5-fluoro-1-(4-methylbenzyl)-2-oxo-2,3-dihydroindol-3-yl]acetic acid, which displayed the highest activity (IC_{50} $0.075 \mu\text{M}$, very close to that of tolrestat IC_{50} $0.046 \mu\text{M}$), with a good selectivity toward ALR2 compared with aldehyde reductase (ALR1) (16.4-fold), and no appreciable inhibitory properties against sorbitol dehydrogenase (SD), or glutathione reductase (GR). The isopropyl ester **59**, a prodrug of **55**, was found to be almost as effective as tolrestat in preventing cataract development in severely galactosemic rats when administered as an eye drop solution. Docking simulation of **55** into a three-dimensional model of human ALR2 made it possible to formulate the hypothesis that the 2-hydroxy tautomer was the active species binding into the catalytic site of the enzyme. This was fully consistent with the structure–activity relationships within this series of cyanooxindolyacetic acid derivatives.

Introduction

Progression of chronic diabetes results in long-term complications, which include neuropathy, nephropathy, retinopathy and cataract formation. In the tissues implicated in these pathologies, the excess of free glucose increases its flux through the polyol pathway leading to an excessive sorbitol production, which is thought to cause cellular damage as a result of osmotic imbalance. Aldose reductase (alditol:NADP⁺ oxidoreductase, EC 1.1.1.21, ALR2) is the first enzyme of the polyol pathway and catalyzes the reduction of glucose by NADPH to sorbitol, which can in turn be oxidized by the enzyme sorbitol dehydrogenase (L-iditol:NAD⁺ 5-oxidoreductase, EC 1.1.1.14, SD) and by NAD⁺ to fructose. Experimental studies in diabetic animals and men have shown that aldose reductase inhibitors (ARIs), which block the flux of the glucose through the polyol pathway and prevent the intracellular accumulation of sorbitol, can prevent, retard, or reverse the complications of chronic diabetes.^{1–5}

Over the past three decades, several ARIs with diverse structures have been discovered. The structural classes exhibiting the most potent activity are the spirohydantoin, whose prototype is sorbinil, and the acetic acid compounds, such as zopolrestat, tolrestat, alrestatin, and epalrestat (Chart 1).^{3,6} However, many of these compounds have failed clinically due to inadequate

Chart 1



* To whom all correspondence should be addressed. Tel: 39 50 500209. Fax: 39 50 40517. E-mail: fsettimo@farm.unipi.it.

[§] Dipartimento di Scienze Farmaceutiche, Università di Pisa.

[‡] Dipartimento di Chimica Farmaceutica e Tossicologica, Università "Federico II" di Napoli.

[†] Farmigea S.p.A.

efficacy, adverse pharmacokinetic properties or toxic side-effects.⁵ For these reasons, there is still a need to

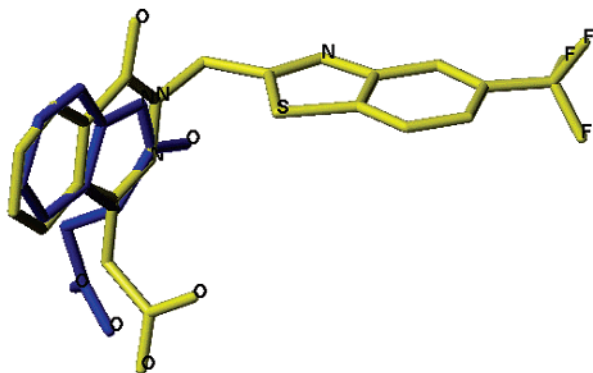


Figure 1. Superimposition of indole derivative **60** (blue) and ALR2-bound conformation of zopolrestat (yellow). Note that the carboxy groups point, in the two structures, toward different directions.

identify and develop clinically effective and well-tolerated ARIs.

We have recently described a new class of selective ARIs: the acetic acid derivatives of [1,2,4]triazino[4,3-*a*]benzimidazole (TBI).⁷ The 10-benzyl TBI derivative (Chart 1) displayed a high inhibitory activity (IC_{50} 0.36 μ M) and was found to be effective in preventing cataract development in severely galactosemic rats when administered as an eye drop solution.

As part of an ongoing effort to identify potent and selective ARIs, in view of our long experience in indole chemistry,^{8–11} we decided to support the acetic acid residue, essential for the inhibition of the enzyme, with the 2-oxoindole nucleus. It has been reported in the literature that potent *in vitro* inhibition of ALR2 has been observed with a number of acetic acid¹² or spirohydantoin¹³ derivatives of oxoindole. At first, following a published procedure,¹⁴ we prepared the 2-oxoindol-3-ylacetic acid **60** (Chart 1) and evaluated its ALR2 inhibitory activity. This compound showed only a low potency, displaying an IC_{50} value of 10^{-4} M.

Actually, molecular modeling studies revealed that compound **60** does not have an excellent overlap with the ALR2-bound conformation of zopolrestat¹⁵ about the carboxylic groups (Figure 1).

Accordingly, we designed the conformationally constrained 2-oxoindolylcyanoacetic acid **39**^{16,17} characterized by a coplanar arrangement of the acetic acid chain with respect to the indole nucleus. As shown in Figure 2, the superposition of **39** (arbitrarily modeled as its *R* enantiomer), TBI, and zopolrestat is quite satisfactory as regards the acetic acid chains and the indole/TBI/phthalazine systems. The match of the fused-benzene rings of **39** and TBI suggests that these moieties might occupy the same domain into the enzyme active site.

A substructure search in the Cambridge Structural Database (CSD)¹⁸ confirmed the rationale of our design: the retrieved crystal structure of ethyl *Z*-1-carboethoxy-2-hydroxy-3-indolylidenecyanoacetate **61** (reference code layjie, Chart 1),¹⁹ a tautomeric form of the 2-oxoindol-3-ylacetic system, exhibits a nearly total coplanar arrangement of the cyanoacetic acid fragment with the indole ring. The attachment of a cyano group on the α -carbon of the acetic acid residue helps to increase the coplanarity of the two moieties owing to the π -conjugation present along the entire system. Subsequent preparation and testing of **39** revealed that

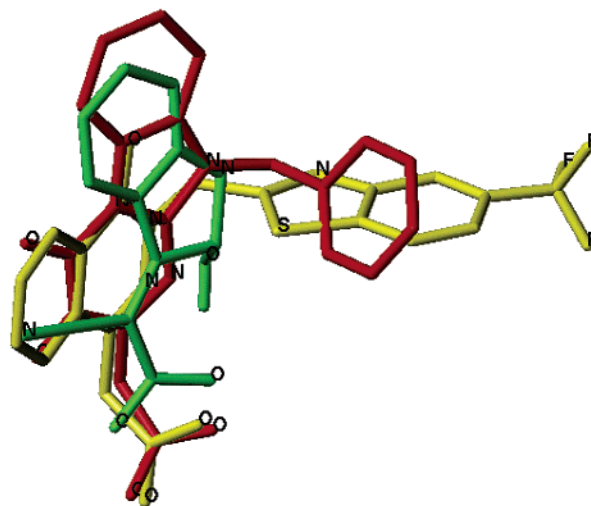


Figure 2. Overlay of **39** (green) on the experimentally determined ALR2-bound conformation of zopolrestat (yellow) and TBI derivative (red).

the ALR2 inhibitory activity was indeed improved by 3 orders of magnitude with respect to that of **60**.

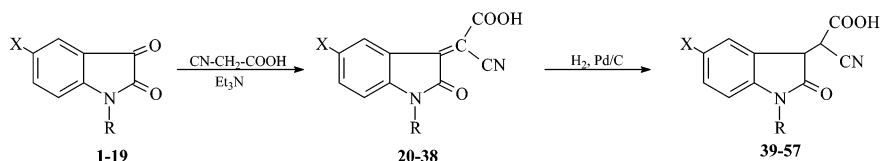
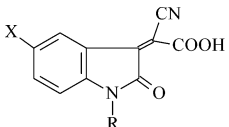
In this paper we describe the synthesis and the biological evaluation of a series of cyano(2-oxo-2,3-dihydroindol-3-yl)acetic acid derivatives (**39–57**). Compound **55**, the most active ALR2 inhibitor among those examined, and its isopropyl ester **59** were also investigated *in vivo* for their ability to prevent cataract development in galactosemic rats. Finally, docking simulations of **55** into the human ALR2 binding site were carried out to rationalize the structure–activity relationships (SARs) observed and to guide, prospectively, the design of new analogues.

Chemistry

The synthesis of the title compounds was performed as outlined in Scheme 1, following a procedure previously reported for derivative **39**.^{16,20} The appropriately substituted isatins **1–19** were condensed with cyanoacetic acid in dioxane solution, in the presence of triethylamine to give the indolidene intermediates **20–38**, which were isolated as an *E–Z* diastereomeric mixtures (Table 1). These mixtures were used directly in the following reaction of hydrogenation, performed in the presence of 10% Pd/C as a catalyst, to obtain the target acids **39–57**. All compounds thus prepared were characterized as diastereomeric mixtures (Table 2). The starting substituted isatins **6–19**, with the exception of the commercially available ones **1–5**, were prepared in accordance with a literature procedure involving the alkylation of isatin **1**, 5-fluoroisatin **2**, or 5-bromoisatin **3** with the appropriate benzyl halide in DMF solution, in the presence of sodium hydride.²¹

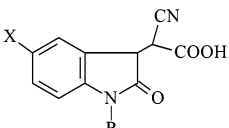
To improve the ocular bioavailability of carboxylic acid **55**, the more lipophilic ester **59** was also prepared. The 5-fluoro-1-(4-methylbenzyl)isatin **17** was converted with a good yield to the diastereomeric mixture of the indolidene intermediate **58** by reaction with isopropyl cyanoacetate in refluxing isopropyl alcohol in the presence of piperidine. Hydrogenation of **58** over 10% Pd/C in an ethanolic solution provided the desired ester **59** as a diastereomeric mixture (Scheme 2; Experimental Section).

Scheme 1

**Table 1.** Physical Properties of Cyano(2-oxo-2,3-dihydroindol-3-ylidene)acetic Acid Derivatives **20–38**


no.	X	R	yield (%)	recrystallization solvent	mp (°C)	formula ^a
20	H	H	50	ethanol	177–180 dec ^b	C ₁₁ H ₆ N ₂ O ₃
21	F	H	98	ethanol/H ₂ O	167–170	C ₁₁ H ₅ FN ₂ O ₃
22	Br	H	70	methanol	242–245	C ₁₁ H ₅ BrN ₂ O ₃
23	NO ₂	H	96	methanol	287–290	C ₁₁ H ₅ N ₃ O ₅
24	OCH ₃	H	42	methanol	188–192 dec ^c	C ₁₂ H ₈ N ₂ O ₄
25	H	CH ₂ C ₆ H ₅	43	ethanol	185–189	C ₁₈ H ₁₂ N ₂ O ₃
26	H	CH ₂ C ₆ H ₄ -p-F	67	ethanol	175–179	C ₁₈ H ₁₁ FN ₂ O ₃
27	H	CH ₂ C ₆ H ₄ -p-CF ₃	81	ethanol	165–168	C ₁₉ H ₁₁ F ₃ N ₂ O ₃
28	H	CH ₂ C ₆ H ₄ -p-CH ₃	73	ethanol	172–175	C ₁₉ H ₁₄ N ₂ O ₃
29	H	CH ₂ C ₆ H ₄ -p-OCH ₃	57	ethanol	148–152 dec	C ₁₉ H ₁₄ N ₂ O ₄
30	F	CH ₃	94	methanol	126–130 dec	C ₁₂ H ₇ FN ₂ O ₃
31	F	CH ₂ CH ₂ Cl	77	methanol	154–157 dec	C ₁₃ H ₈ ClFN ₂ O ₃
32	F	CH ₂ CH ₂ CH ₃	81	methanol	160–163 dec	C ₁₄ H ₁₁ FN ₂ O ₃
33	F	CH ₂ C ₆ H ₅	41	ethanol	146–148	C ₁₈ H ₁₁ FN ₂ O ₃
34	F	CH ₂ C ₆ H ₄ -p-F	85	ethanol	155–157	C ₁₈ H ₁₀ F ₂ N ₂ O ₃
35	F	CH ₂ C ₆ H ₄ -p-CF ₃	61	ethanol	157–160	C ₁₉ H ₁₀ F ₄ N ₂ O ₃
36	F	CH ₂ C ₆ H ₄ -p-CH ₃	83	ethanol	168–171	C ₁₉ H ₁₃ FN ₂ O ₃
37	F	CH ₂ C ₆ H ₄ -p-OCH ₃	58	ethanol	167–169	C ₁₉ H ₁₃ FN ₂ O ₄
38	Br	CH ₂ C ₆ H ₄ -p-CH ₃	36	methanol	127–128 dec	C ₁₉ H ₁₃ BrN ₂ O ₃

^a Elemental analyses for C, H, N were within $\pm 0.4\%$ of the calculated value. ^b Lit.¹⁶ mp: 172 °C. ^c Lit.⁴⁰ mp: 185–186.

Table 2. Physical Properties and Inhibition of ALR2 by Cyano(2-oxo-2,3-dihydroindol-3-yl)acetic Acid Derivatives **39–57**


no.	X	R	yield (%)	recrystallization solvent	mp (°C)	formula ^a	IC ₅₀ ^b (μM)
39	H	H	47	EtOAc	179–182 dec ^c	C ₁₁ H ₈ N ₂ O ₃	0.85 (0.59–1.10)
40	F	H	30	EtOAc/petroleum ether 60–80 °C	178–180	C ₁₁ H ₇ FN ₂ O ₃	0.28 (0.20–0.38)
41	Br	H	74	EtOAc	150–154	C ₁₁ H ₇ BrN ₂ O ₃	0.38 (0.25–0.49)
42	NO ₂	H	27	CH ₂ Cl ₂	177–180	C ₁₁ H ₇ N ₃ O ₅	1.20 (0.94–1.46)
43	OCH ₃	H	50	EtOAc	107–110 ^d	C ₁₂ H ₁₀ N ₂ O ₄	5.40 (3.90–7.06)
44	H	CH ₂ C ₆ H ₅	33	CH ₂ Cl ₂	126–130	C ₁₈ H ₁₄ N ₂ O ₃	3.20 (2.44–4.16)
45	H	CH ₂ C ₆ H ₄ -p-F	27	CH ₂ Cl ₂	157–160	C ₁₈ H ₁₃ FN ₂ O ₃	0.57 (0.40–0.74)
46	H	CH ₂ C ₆ H ₄ -p-CF ₃	23	CH ₂ Cl ₂ /petroleum ether 60–80 °C	151–154	C ₁₉ H ₁₃ F ₃ N ₂ O ₃	0.57 (0.43–0.69)
47	H	CH ₂ C ₆ H ₄ -p-CH ₃	38	EtOAc/petroleum ether 60–80 °C	169–172	C ₁₉ H ₁₆ N ₂ O ₃	0.64 (0.44–0.88)
48	H	CH ₂ C ₆ H ₄ -p-OCH ₃	40	CH ₂ Cl ₂ /petroleum ether 60–80 °C	149–152	C ₁₉ H ₁₆ N ₂ O ₄	0.63 (0.44–0.80)
49	F	CH ₃	62	EtOAc/petroleum ether 60–80 °C	170–174	C ₁₂ H ₉ FN ₂ O ₃	0.39 (0.32–0.47)
50	F	CH ₂ CH ₂ Cl	74	EtOAc/petroleum ether 40–60 °C	87–90	C ₁₃ H ₁₀ ClFN ₂ O ₃	1.34 (0.92–1.74)
51	F	CH ₂ CH ₂ CH ₃	64	EtOAc/petroleum ether 40–60 °C	97–100	C ₁₄ H ₁₃ FN ₂ O ₃	0.28 (0.22–0.35)
52	F	CH ₂ C ₆ H ₅	13	CH ₂ Cl ₂ /petroleum ether 60–80 °C	168–172	C ₁₈ H ₁₃ FN ₂ O ₃	0.18 (0.12–0.22)
53	F	CH ₂ C ₆ H ₄ -p-F	32	CH ₂ Cl ₂ /petroleum ether 60–80 °C	149–152	C ₁₈ H ₁₂ F ₂ N ₂ O ₃	0.13 (0.09–0.17)
54	F	CH ₂ C ₆ H ₄ -p-CF ₃	65	EtOAc/petroleum ether 60–80 °C	80–81	C ₁₉ H ₁₀ F ₄ N ₂ O ₃	0.28 (0.23–0.35)
55	F	CH ₂ C ₆ H ₄ -p-CH ₃	45	EtOAc/petroleum ether 60–80 °C	173–176	C ₁₉ H ₁₅ FN ₂ O ₃	0.075 (0.059–0.090)
56	F	CH ₂ C ₆ H ₄ -p-OCH ₃	25	CH ₂ Cl ₂ /petroleum ether 60–80 °C	166–169	C ₁₉ H ₁₅ FN ₂ O ₄	0.11 (0.08–0.13)
57	Br	CH ₂ C ₆ H ₄ -p-CH ₃	71	CH ₂ Cl ₂	167–171	C ₁₉ H ₁₅ BrN ₂ O ₃	0.25 (0.19–0.30)
sorbinil							0.50 (0.39–0.62)
tolrestat							0.046 (0.036–0.055)
quercetin							8.32 (6.90–9.91)

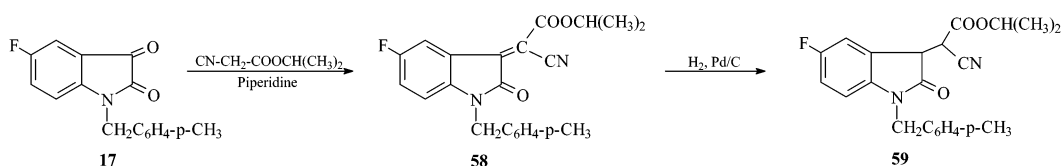
^a Elemental analyses for C, H, N were within $\pm 0.4\%$ of the calculated value. ^b IC₅₀ values represent the concentration required to produce 50% enzyme inhibition. ^c Lit.¹⁶ mp: 179 °C. ^d Lit.⁴⁰ mp 164–165 °C.

Biology and Pharmacology

The diastereomeric mixtures of the target compounds **39–57** were used as such to evaluate their *in vitro* inhibitory activity against ALR2. Primary *in vitro* screening was performed on a water-soluble crude

enzymatic extract of rat lenses.^{22–25} IC₅₀ values were determined by using linear regression analysis of the log concentration–response curve. Sorbinil,²⁶ tolrestat,^{27,28} and quercetin²⁹ were used as the reference standards. Selected compounds (**40**, **47**, **53**, **55**), which

Scheme 2

**Table 3.** Enzyme Inhibition Data of Selected Compounds **40**, **47**, **53**, and **55**

no.	aldose reductase IC ₅₀ ^a (μM)	aldehyde reductase IC ₅₀ ^a (μM)	sorbitol dehydrogenase IC ₅₀ ^a (μM)	glutathione reductase IC ₅₀ ^a (μM)
40	0.28 (0.19–0.37)	6.79 (4.75–8.82)	n.a. ^b	n.a.
47	0.46 (0.32–0.69)	3.57 (2.50–4.64)	n.a.	n.a.
53	0.058 (0.044–0.071)	0.49 (0.31–0.63)	n.a.	n.a.
55	0.042 (0.030–0.055)	0.69 (0.48–0.89)	n.a.	n.a.
sorbinil	0.65 (0.49–0.82)	0.029 (0.020–0.038)	n.a.	n.a.
tolrestat	0.05 (0.03–0.06)	n.a.	n.a.	n.a.
quercetin	7.81 (5.47–10.15)	2.32 (2.05–2.78)	35.6 (31.6–40.0)	48.8 (34.7–63.4)

^a IC₅₀ values represent the concentration required to produce 50% enzyme inhibition. ^b n.a. = not active.

demonstrated significant inhibitory activity, were assayed for their ability to inhibit ALR2 purified from rat lenses, SD,³⁰ and two other enzymes not involved in the polyol pathway, namely aldehyde reductase (ALR1),³¹ and glutathione reductase (GR).³²

The most active derivative **55** and its isopropyl ester **59** were investigated in vivo as eye drop solutions in the precorneal region for their ability to prevent cataract development in severely galactosemic rats.²⁶ Their effectiveness was evaluated with respect to tolrestat as a highly potent reversible inhibitor of lenticular ALR2 when topically administered to rats fed with 50% galactose diet.²⁸

Results and Discussion

Biological Evaluation. To deduce sound structure–activity relationships, IC₅₀s should on principle be determined on pure inhibitors. One drawback of testing mixtures of stereoisomers, unavoidable in our case, was that we could not assess how each stereoisomer affected the enzyme. On the other hand, the IC₅₀ values calculated can be used as a screening method to select promising inhibitors and to identify the diastereomeric mixture with the best ability to inhibit the enzyme. All the cyanoindolylacetic acids **39–57** exhibited a high inhibitory activity, with IC₅₀ values in the low/sub-micromolar range (Table 2). In the series of the 1-unsubstituted derivatives **39–43**, the best potency was shown by the 5-halo compounds **40** and **41**. All the 5-H indoles, substituted with a lipophilic area on the indole nitrogen (**44–48**), demonstrated almost the same inhibitory potency, **44** being the only exception. The 5-F and 5-Br derivatives **49–57** displayed the best ability to inhibit ALR2, with compound **55** being the most potent inhibitor of the whole series, showing an IC₅₀ value (0.075 μM) similar to that of tolrestat (0.046 μM), and lower than that of sorbinil (0.50 μM).

Finally, the selected compounds **40**, **47**, **53**, and **55**, when assayed for their ability to inhibit purified ALR2 and other related enzymes (ALR1, SD, and GR), were all found to be selective inhibitors of ALR2, inhibiting ALR1 with much less potency (from 8- to 24-fold), and showing no appreciable inhibitory properties toward SD, or GR (Table 3).

Pharmacological Evaluation of Compounds 55 and 59. Compound **55** was administered as an eyedrop

Table 4. Effect of Treatment with Ophthalmic Solution of **55**, **59**, and Tolrestat on Development of Nuclear Cataract in Severely Galactosemic Rats

day of treatment	rats with nuclear cataract (%)				
	control	55 (3%)	59 (3%)	tolrestat (1%)	tolrestat (3%)
11	13	0	0	0	0
12	25	0	0	0	0
13	25	0	0	0	0
14	25	18	0	23	0
15	25	43	0	32	0
16	31	57	0	32	0
17	50	57	0	32	0
18	50	72	0	43	0
19	75	84	8	43	0
20	88	96	8	47	0
21	100	100	8	47	0

solution in the precorneal region to investigate its in vivo ability to prevent cataract development in severely galactosemic rats. Topical administration can in principle achieve significant drug levels in the lens with negligible effects on other tissues, thus avoiding bioavailability and/or metabolism-related problems associated with systemic administration.²⁸ It has been reported^{33–35} that esters of acid drugs display a better corneal permeability and ocular bioavailability by virtue of their higher lipophilicity. Considering that isopropyl esters have shown a good permeability in the corneal tissue,³³ the isopropyl ester **59** was prepared and tested in vivo as a prodrug of compound **55**. The pharmacological data are reported in Table 4. After 21 days of 50% galactose diet, 100% of the animals treated only with vehicle developed nuclear cataract. No protection was observed in those treated with 3% ophthalmic solution of the acid **55**, whereas an almost complete protection was detected in rats treated with 3% solution of the isopropyl ester **59**. No nuclear cataract was developed by animals administered 3% ophthalmic solution of tolrestat. The high potency displayed by the prodrug **59** with respect to the acid **55** suggests that its higher lipophilicity is essential for a good permeability in corneal tissue and that its inhibitory activity is ensured by a quick hydrolysis to the active acid by corneal esterases.

Molecular Modeling. Derivatives **39–57** are capable of tautomeric isomerism, as shown in Figure 3.

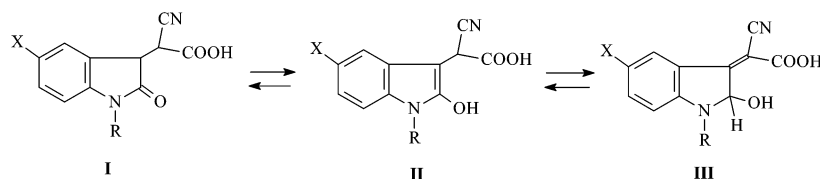


Figure 3. Tautomeric equilibria of cyano(2-oxo-2,3-dihydroindol-3-yl)acetic acid derivatives **39–57**.

The ^1H NMR spectrum of **55** recorded in dimethyl sulfoxide, a polar nonprotic solvent, showed the presence of only the carbonyl form **I**. Nothing can be said about the tautomeric form present in water solution, since with deuterium oxide the two signals relative to the H-3 and the acetic CH disappeared, showing that their acidity/mobility was certainly due to the equilibrium among the three tautomeric forms.

However, the most stable tautomer in the gas or solution phases is not necessarily the one preferred by the enzyme. We hypothesize that our compounds bind to the enzyme in the hydroxy form **III** because this tautomer is not only better superimposable on the ALR2-bound conformation of zopolrestat (Figure 2), but it also fits nicely into the inhibitory site (see below). Moreover, the crystal structure of the cyanoacetate derivative **61**¹⁹ (Chart 1), structurally similar to **55**, is frozen in the hydroxy form **III**, thus suggesting that this tautomeric arrangement is energetically feasible. This tautomer receives further stabilization from an intramolecular hydrogen bond formed between the 2-hydroxy group and one of the two carboxylate oxygens.

Even though the IC_{50} values were from diastereomeric mixtures, we thought it interesting to rationalize the results obtained within this series of cyano derivatives, and to formulate a hypothesis about their binding mode at the active site of the enzyme. For this purpose, we docked the most potent inhibitor **55** (frozen in the hydroxy tautomeric form **III**) into the previously modeled structure of human ALR2.⁷

The bioactive conformation of the TBI derivative⁷ and the experimentally determined ALR2-bound conformation of zopolrestat¹⁵ served as templates to select a trial conformation of **55** for docking calculations. By manual adjustment of the torsional angles τ_1 , τ_2 , and τ_3 (defined in Figure 4), we identified a low-energy conformation of **55** superimposable on TBI and zopolrestat about the carboxylic acid groups and the *p*-tolyl/phenyl/benzothiazole moieties.

Both *R* and *S* enantiomers of the cyanoindolylacetic derivative **55** were considered for docking, because all the investigated compounds were assayed as racemic mixtures. These enantiomers are isoenergetic and differ only in the position of the 2-hydroxy group, which may project above or below the plane of the ligand, giving rise in both cases to a hydrogen bond with one of the two carboxylate oxygen atoms.

Docking was carried out using the automated DOCK software package,^{36–39} following the same protocol described in a previous paper.⁷ Interestingly, the best-scoring docking orientation of both (*R*)-**55** and (*S*)-**55** yielded the most satisfactory superposition on the ALR2-bound conformation of zopolrestat.

The geometries of the ALR2/NADP⁺/(*R*)-**55** and ALR2/NADP⁺/(*S*)-**55** complexes were refined by extensive energy minimization and molecular dynamics (MD)

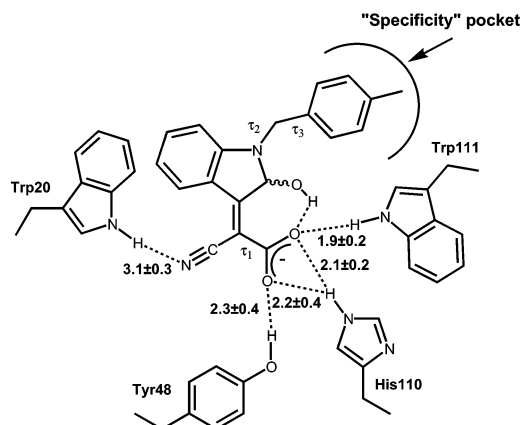


Figure 4. Schematic representation of the main interactions observed in the MD simulation of the ALR2/NADP⁺/**55** complex. The interatomic distances are given as mean values of those observed during the MD simulation, accompanied by standard deviation.

simulations in a solvated system at room temperature in order to relieve steric repulsive conflicts between the flexible amino acid side chains of the enzyme and the docked ligand.

General binding features are schematically represented in Figure 4 together with interatomic distances for all important polar interactions. Details of the binding mode of the two enantiomers are shown in Figure 5, where only the amino acids located within 5 Å of the bound ligand are depicted.

As the degree of stereoelectronic complementarity between the docked enantiomers and the enzyme, estimated on the basis of the interaction energies, was rather similar, we predict that the enantiomers of each inhibitor should not exhibit significant differences in potency.

As illustrated in Figure 4, the negatively charged carboxylate group of the cyano derivative **55** makes a tight hydrogen-bonding network with Tyr48, His110, and Trp111 of ALR2. Particularly, the N^{ε2} hydrogen of His110 is hydrogen-bonded to both of the carboxylate oxygen atoms O² and O³, while the O^γ hydrogen of Tyr48 and the N^{ε1} hydrogen of Trp111 form a hydrogen bond with each of the two carboxylate oxygens. Coordination of the inhibitor's carboxylate group to the anionic binding site was maintained for the entire simulation time, suggesting that this group is the primary determinant for binding of **55** and its derivatives. Another favorable interaction between the cyano nitrogen atom of the ligand and the N^{ε1} hydrogen of Trp20 was also shown to contribute to the complex stabilization, although it was observed to be frequently cleaved in the simulation, giving an average distance longer than that for an ideal hydrogen bond.

The *p*-tolyl moiety of **55** fits into the specificity pocket made up of four aromatic residues (Trp79, Trp111,

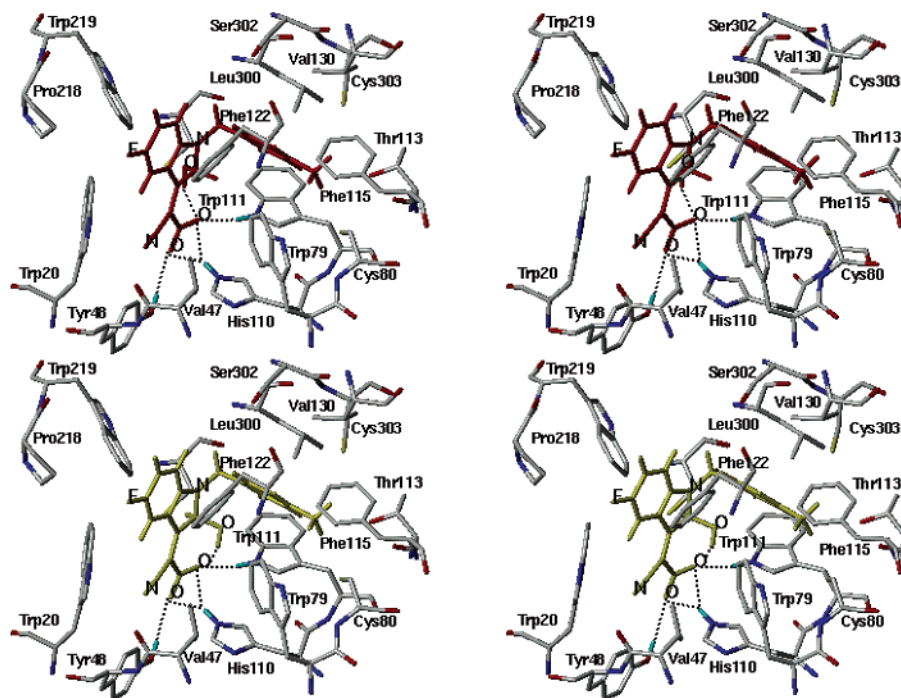


Figure 5. (*R*)-**55** (top) and (*S*)-**55** (bottom) enantiomers docked into the ALR2 binding site. Only amino acids located within 5 Å distance from the bound ligand are displayed and labeled. The hydrogen bonds discussed in the text are depicted as black dashed lines.

Phe115, and Phe122), two nonpolar residues (Val130, Leu300) and five polar residues (Cys80, Thr113, Cys298, Ser302, Cys303) (Figure 5).

Phe122 and Trp219 are involved in hydrophobic contacts with the indole nucleus of the inhibitor. Particularly, the benzene ring of Phe122 appears to be optimally oriented for a favorable π -stacking interaction with the fused aromatic ring of **55**: the planes of the two rings are fairly parallel and separated by a distance of 4.7 Å. The Trp219 side chain also interacts with the fused aromatic ring of the inhibitor via a T-shaped interaction. Such interactions would be consistent with the activity trend of these compounds showing that lipophilic and electron-withdrawing substituents in the 5-position of the indole nucleus increase the potency. In fact, the electron-deficient halogenated fused ring of indole would more favorably realize a π -stacking charge-transfer interaction with the electron-rich ring of Phe122, while the replacement of fluorine or bromine with a nitro group (**42**), which has greater electron-withdrawing nature but less lipophilicity than halogens, decreases activity.

Conclusions

We have described a novel class of highly potent ARIs: the cyano(2-oxo-2,3-dihydroindol-3-yl)acetic acid derivatives. Compound **55**, the most potent derivative of the series, exhibited an ALR2 inhibitory activity (IC_{50} 0.075 μ M) very close to that of tolrestat (IC_{50} 0.046 μ M), with a 16.4-fold higher selectivity toward ALR2 compared with ALR1, and no appreciable inhibitory properties against SD or GR. The isopropyl ester **59**, a prodrug of **55**, proved to be almost as effective as tolrestat in preventing cataract development in severely galactosemic rats when administered as an eye drop solution.

Experimental Section

1. Chemistry. Melting points were determined using a Reichert Kofler hot-stage apparatus and are uncorrected. IR spectra were recorded with a Pye Unicam Infracord Model PU 9516 in Nujol mulls. Routine 1H NMR spectra were determined on a Varian CFT 20 Spectrometer operating at 80 MHz, using tetramethylsilane (TMS) as the internal standard and DMSO- d_6 as the solvent. Mass spectra were obtained on a Hewlett-Packard 5988 A spectrometer using a direct injection probe and an electron beam energy of 70 eV. Evaporations were performed in vacuo (rotary evaporator). Analytical TLC was carried out on Merck 0.2 mm precoated silica gel (60 F-254) aluminum sheets, with visualization by irradiation with a UV lamp. Elemental analyses were performed by our Analytical Laboratory and agreed with theoretical values to within $\pm 0.4\%$.

The alkyl halides 1-iodopropane, 1-bromo-2-chloroethane, benzyl bromide, 4-fluorobenzyl chloride, 4-methylbenzyl bromide, 4-(trifluoromethyl)benzyl bromide, and 4-methoxybenzyl chloride used to obtain compounds **13**, **12**, **14**, **7**, **15**, **17**, **19**, **8**, **16**, **18**, respectively, and isatin **1**, 5-fluoroisatin **2**, 5-bromoisatin **3**, 5-nitroisatin **4**, were from Sigma-Aldrich.

The following products were prepared in accordance with literature procedures: 5-methoxyisatin **5**, mp 198–201 °C (lit.⁴⁰ mp 202 °C); 1-benzylisatin **6**, mp 130–131 °C (lit.⁴¹ mp 131–131.5 °C); 1-(4-methylbenzyl)isatin **9**, mp 142–143 °C (lit.⁴¹ mp 141 °C); 1-(4-methoxybenzyl)isatin **10**, mp 168–170 °C (lit.⁴² mp 171–172 °C); 5-fluoro-1-methylisatin **11**, mp 157–159 °C (lit.⁴³ mp 151 °C); 2-oxoindol-3-ylacetic acid **60**, mp 142–144 °C (lit.¹⁴ mp 140–142 °C).

General Procedure for the Synthesis of 1-Alkylisatins 7, 8 and 5-Substituted-1-alkylisatins 12–19. Sodium hydride (12 mmol, 50% dispersion in mineral oil) was added portionwise, under a nitrogen atmosphere, to an ice-cooled solution of isatin **1**, 5-fluoroisatin **2**, or 5-bromoisatin **3** (10 mmol) in 5 mL of freshly distilled DMF. Once hydrogen evolution had ceased, the appropriate alkyl halide (12 mmol) was added dropwise, and the reaction mixture was maintained under stirring, at room temperature, until the disappearance of the starting material (0.5–3 h, TLC analysis). The solution was then slowly poured onto crushed ice, and the solid

precipitate was collected, washed with water, and recrystallized. Yields, recrystallization solvents, melting points, and spectral data for the newly synthesized compounds are listed below.

1-(4-Fluorobenzyl)isatin 7. mp 148–149 °C (ethanol); yield 52%. IR ν cm^{-1} : 1720, 1600. ^1H NMR δ , CDCl_3 : 4.87 (s, 2H, CH_2); 6.69–7.62 (m, 8H, ArH). Anal. ($\text{C}_{15}\text{H}_{10}\text{FNO}_2$) C, H, N.

1-(4-Trifluoromethylbenzyl)isatin 8. mp 120–121 °C (toluene); yield 35%. IR ν cm^{-1} : 1740, 1720, 1600. ^1H NMR δ , CDCl_3 : 5.06 (s, 2H, CH_2); 6.75–7.74 (m, 8H, ArH). Anal. ($\text{C}_{16}\text{H}_{10}\text{F}_3\text{NO}_2$) C, H, N.

1-(2-Chloroethyl)-5-fluoroisatin 12. mp 101–102 °C (petroleum ether 60–80 °C); yield 88%. IR ν cm^{-1} : 1730, 1610. ^1H NMR δ : 3.84 (t, 2H, NCH_2); 4.05 (t, 2H, CH_2Cl); 7.30–7.60 (m, 3H, ArH). Anal. ($\text{C}_{10}\text{H}_7\text{ClFNO}_2$) C, H, N.

5-Fluoro-1-*n*-propylisatin 13. mp 80–81 °C (petroleum ether 60–80 °C); yield 85%. IR ν cm^{-1} : 1730, 1610. ^1H NMR δ : 0.89 (t, 3H, CH_3); 1.54–1.65 (m, 2H, CH_2); 3.61 (t, 2H, NCH_2); 7.19–7.56 (m, 3H, ArH). Anal. ($\text{C}_{11}\text{H}_{10}\text{FNO}_2$) C, H, N.

1-Benzyl-5-fluoroisatin 14. mp 131–132 °C (ethanol); yield 51%. IR ν cm^{-1} : 1740, 1700, 1620, 1610. ^1H NMR δ , CDCl_3 : 4.90 (s, 2H, CH_2); 6.73–7.36 (m, 8H, ArH). Anal. ($\text{C}_{15}\text{H}_{10}\text{FNO}_2$) C, H, N.

5-Fluoro-1-(4-fluorobenzyl)isatin 15. mp 157–158 °C (petroleum ether 60–80 °C); yield 44%. IR ν cm^{-1} : 1740, 1720, 1620, 1600. ^1H NMR δ , CDCl_3 : 4.88 (s, 2H, CH_2); 6.61–7.37 (m, 7H, ArH). Anal. ($\text{C}_{15}\text{H}_9\text{F}_2\text{NO}_2$) C, H, N.

5-Fluoro-1-(4-trifluoromethylbenzyl)isatin 16. mp 117–118 °C (ethyl acetate/petroleum ether 60–80 °C); yield 45%. IR ν cm^{-1} : 1730, 1710, 1600. ^1H NMR δ : 4.96 (s, 2H, CH_2); 6.58–7.64 (m, 7H, ArH). Anal. ($\text{C}_{16}\text{H}_9\text{F}_4\text{NO}_2$) C, H, N.

5-Fluoro-1-(4-methylbenzyl)isatin 17. mp 140–141 °C (petroleum ether 60–80 °C); yield 54%. IR ν cm^{-1} : 1740, 1720, 1600. ^1H NMR δ : 2.31 (s, 3H, CH_3); 4.85 (s, 2H, CH_2); 6.61–7.40 (m, 7H, ArH). Anal. ($\text{C}_{16}\text{H}_{12}\text{FNO}_2$) C, H, N.

5-Fluoro-1-(4-methoxybenzyl)isatin 18. mp 134–137 °C (ethanol); yield 48%. IR ν cm^{-1} : 1720, 1600. ^1H NMR δ , CDCl_3 : 3.76 (s, 3H, CH_3); 4.83 (s, 2H, CH_2); 6.63–7.31 (m, 7H, ArH). Anal. ($\text{C}_{16}\text{H}_{12}\text{FNO}_3$) C, H, N.

5-Bromo-1-(4-methylbenzyl)isatin 19. mp 156–158 °C (ethyl acetate); yield 75%. IR ν cm^{-1} : 1780, 1760, 1630. ^1H NMR δ : 2.26 (s, 3H, CH_3); 4.84 (s, 2H, CH_2); 6.85–7.76 (m, 7H, ArH). Anal. ($\text{C}_{16}\text{H}_{12}\text{BrNO}_2$) C, H, N.

General Procedure for the Synthesis of Cyano(2-oxo-2,3-dihydroindol-3-ylidene)acetic Acids 20–38. A solution of cyanoacetic acid (1.02 g, 12 mmol) and triethylamine (1.7 mL, 12 mmol) in dioxane (10 mL) was added dropwise to an ice-cooled suspension of the appropriate isatin 1–19 (10 mmol) in dioxane (10 mL). Once addition was complete, stirring was continued at room temperature until the disappearance of the starting material (2–4 h, TLC analysis). Then, concentrated hydrochloric acid (0.3 mL) was added slowly, under stirring and with cooling, to the dark red reaction mixture. The resulting solution was left at room temperature for 5–6 days until the crude product separated. The precipitate was collected, washed with water, and recrystallized from the appropriate solvent. Yields, recrystallization solvents, and melting points of the target compounds, characterized as an *E–Z* diastereomeric mixture, are reported in Table 1. The spectral data for **21** and **28**, which are representative for the title compounds, are listed below.

Cyano(5-fluoro-2-oxo-2,3-dihydroindol-3-ylidene)acetic Acid 21. IR ν cm^{-1} : 3350, 3200–2400, 2200, 1700, 1620, 1560. ^1H NMR δ : 6.75–7.97 (m, 3H, ArH); 10.96 (s, 1H, NH).

Cyano[5-fluoro-1-(4-methylbenzyl)-2-oxo-2,3-dihydroindol-3-ylidene]acetic Acid 28. IR ν cm^{-1} : 3250–2600, 2200, 1700, 1600, 1560. ^1H NMR δ : 2.25 (s, 3H, CH_3); 4.87 (s, 2H, CH_2); 6.74–8.03 (m, 7H, ArH).

General Procedure for the Synthesis of Cyano(2-oxo-2,3-dihydroindol-3-yl)acetic Acids 39–57. A solution of the appropriate acid **20–38** (1 mmol) in absolute ethanol (10 mL) was hydrogenated with 10% Pd/C as a catalyst at atmospheric pressure and room temperature until the theoretical uptake

of hydrogen was achieved (in the case of the 5-nitro derivative **23** the reduction reaction was stopped after the absorption of 1 mol of hydrogen). The catalyst was then filtered off, and the solvent was evaporated to dryness under reduced pressure to obtain an oily residue which solidified by treatment with ice-cooled petroleum ether (40–60 °C or 60–80 °C). The crude solid was collected and recrystallized from the appropriate solvent. Yields, recrystallization solvents, and melting points of the products, characterized as diastereomeric mixtures, are reported in Table 2. The spectral data of **53** and **55**, which are representative of the title compounds, are listed below.

Cyano[5-fluoro-1-(4-fluorobenzyl)-2-oxo-2,3-dihydroindol-3-yl]acetic Acid 53. IR ν cm^{-1} : 3220–2250, 2200, 1720, 1640. ^1H NMR δ : 4.20–4.46 (m, 1H, 3-H, exch. with D_2O); 4.87, 4.92 (2s, 2H, CH_2); 4.97–5.07 (m, 1H, CHCOOH , exch. with D_2O); 6.76–7.47 (m, 7H, ArH).

Cyano[5-fluoro-1-(4-methylbenzyl)-2-oxo-2,3-dihydroindol-3-yl]acetic Acid 55. IR ν cm^{-1} : 3200–2400, 2275, 1750, 1640. ^1H NMR δ : 2.25 (s, 3H, CH_3); 4.36–4.44 (m, 1H, 3-H, exch. with D_2O); 4.81, 4.87 (2s, 2H, CH_2); 4.94–5.06 (m, 1H, CHCOOH , exch. with D_2O); 6.69–7.35 (m, 7H, ArH).

Cyano[5-fluoro-1-(4-methylbenzyl)-2-oxo-2,3-dihydroindol-3-ylidene]acetic Acid Isopropyl Ester 58. A suspension of 5-fluoro-1-(4-methylbenzyl)isatin **17** (0.269 g, 1 mmol) and isopropyl cyanoacetate (0.15 mL, 1.2 mmol) in isopropyl alcohol (5 mL) containing piperidine (0.12 mL, 1.2 mmol) was heated under reflux for 15 min. After cooling, a deep purple solid separated, which was collected and recrystallized from isopropyl alcohol to give 0.226 g (yield 60%) of pure **58** as an *E–Z* diastereomeric mixture. mp 182–184 °C. IR, ν cm^{-1} : 1710, 1280, 1260. ^1H NMR, δ : 1.34 (d, 6H, $\text{CH}(\text{CH}_3)_2$); 2.25 (s, 3H, CH_3); 4.88 (s, 2H, CH_2); 5.18–5.21 (m, 1H, CH); 6.97–8.05 (m, 7H, ArH). MS: *m/e* 378 (M^+), 105, base. Anal. ($\text{C}_{22}\text{H}_{19}\text{FN}_2\text{O}_3$) C, H, N.

Cyano[5-fluoro-1-(4-methylbenzyl)-2-oxo-2,3-dihydroindol-3-yl]acetic Acid Isopropyl Ester 59. A solution of the ester **58** (0.378 g, 1 mmol) in isopropyl alcohol (10 mL) was hydrogenated with 10% Pd/C as a catalyst at atmospheric pressure and room temperature until the theoretical uptake of hydrogen was achieved. The catalyst was then filtered off, and the solvent was evaporated to dryness under reduced pressure to an oily product which solidified by treatment with ice-cooled petroleum ether 40–60 °C.

The resulting white solid was collected and recrystallized from isopropyl alcohol to obtain 0.304 g (yield 80%) of pure **59** as a diastereomeric mixture. mp 110–112 °C. IR, ν cm^{-1} : 1740, 1700. ^1H NMR, δ : 1.10–1.22 (m, 6H, $\text{CH}(\text{CH}_3)_2$); 2.24 (s, 3H, CH_3); 4.54–5.24 (m, 5H, CH–CH, OCH, NCH_2); 6.88–7.25 (m, 7H, ArH). MS: *m/e* 380 (M^+), 105, base. Anal. ($\text{C}_{22}\text{H}_{21}\text{FN}_2\text{O}_3$) C, H, N.

2. Biology. 2.1. Materials and Methods. Aldose reductase (ALR2) and aldehyde reductase (ALR1) were obtained from Sprague Dawley albino rats, 120–140 g b.w., supplied by Harlan Nossan, Italy. In order to minimize cross-contamination between ALR2 and ALR1 in the enzyme preparation, rat lens, in which ALR2 is the predominant enzyme, and kidney, where ALR1 shows the highest concentration, were used for isolation of ALR2 and ALR1, respectively.

Glutathione reductase (GR) type IV from bakers' yeast (100–300 U/mg), sorbitol dehydrogenase (SD) from sheep liver (10 U/mg of protein), pyridine coenzymes, D,L-glyceraldehyde, glutathione disulfide, sodium D-glucuronate, sorbitol, and quercetin were from Sigma Chemical Co. Sorbinil was a gift from Pfizer, Groton CT. Tolrestat was obtained from Lorestat Recordati, Italy. All other chemicals were of reagent grade.

2.2. Enzyme Preparation. 2.2.1. Aldose Reductase (ALR2). A purified rat lens extract was prepared in accordance with the method of Hayman and Kinoshita⁴⁴ with slight modifications. Lens were quickly removed from normal killed rats and homogenized (Glas-Potter) in 3 volumes of cold deionized water. The homogenate was centrifuged at 12 000 rpm at 0–4 °C for 30 min. Saturated ammonium sulfate solution was added to the supernatant fraction to form a 40% solution, which was stirred for 30 min at 0–4 °C and then

centrifuged at 12 000 rpm for 15 min. Following this same procedure, the recovered supernatant was subsequently fractionated with saturated ammonium sulfate solution using first 50% and then 75% salt saturation. The precipitate recovered from the 75% saturated fraction, containing ALR2 activity, was redissolved in 0.05 M NaCl and dialyzed overnight in 0.05 M NaCl. The dialyzed material was used for the enzymatic assay.

2.2.2. Aldehyde reductase (ALR1). Rat kidney ALR1 was prepared in accordance with a previously reported method.³¹ Kidneys were quickly removed from normal killed rats and homogenized (Glas-Potter) in 3 volumes of 10 mM sodium phosphate buffer, pH = 7.2, containing 0.25 M sucrose, 2.0 mM EDTA dipotassium salt and 2.5 mM β -mercaptoethanol. The homogenate was centrifuged at 12 000 rpm at 0–4 °C for 30 min, and the supernatant was subjected to a 40–75% ammonium sulfate fractionation, following the same procedure previously described for ALR2. The precipitate obtained from the 75% ammonium sulfate saturation, containing ALR1 activity, was redissolved in 50 volumes of 10 mM sodium phosphate buffer, pH = 7.2, containing 2.0 mM EDTA dipotassium salt and 2.0 mM β -mercaptoethanol and dialyzed overnight using the same buffer. The dialyzed material was used in the enzymatic assay.

2.3. Enzymatic Assays. The activity of the four test enzymes was determined spectrophotometrically by monitoring the change in absorbance at 340 nm, which is due to the oxidation of NADPH or the reduction of NAD⁺ catalyzed by ALR2, ALR1, and GR or SD, respectively. The change in pyridine coenzyme concentration/min was determined using a Beckman DU-64 kinetics software program (Solf Pack TM Module).

ALR2 activity was assayed at 30 °C in a reaction mixture containing 0.25 mL of 10 mM d,L-glyceraldehyde, 0.25 mL of 0.104 mM NADPH, 0.25 mL of 0.1 M sodium phosphate buffer (pH = 6.2), 0.1 mL of enzyme extract and 0.15 mL of deionized water in a total volume of 1 mL. All the above reagents, except d,L-glyceraldehyde, were incubated at 30 °C for 10 min; the substrate was then added to start the reaction, which was monitored for 5 min. Enzyme activity was calibrated by diluting the enzymatic solution in order to obtain an average reaction rate of 0.011 ± 0.0010 absorbance units/min for the sample.

ALR1 activity was determined at 37 °C in a reaction mixture containing 0.25 mL of 20 mM sodium D-glucuronate, 0.25 mL of 0.12 mM NADPH, 0.25 mL of dialyzed enzymatic solution, and 0.25 mL of 0.1 M sodium phosphate buffer (pH = 7.2) in a total volume of 1 mL. The enzyme activity was calibrated by diluting the dialyzed enzymatic solution in order to obtain an average reaction rate of 0.015 ± 0.0010 absorbance units/min for the sample.

SD activity³⁰ was determined at 37 °C in a reaction mixture containing 0.25 mL of 10 mM sorbitol, 0.25 mL of 0.47 mM NAD⁺, 0.25 mL of 3.75 mU/mL enzymatic solution, and 0.25 mL of 100 mM TRIS/HCl buffer (pH = 8) in a total volume of 1 mL. All the reagents were incubated at 37 °C for 1 min, after which the reaction was monitored for 3 min.

GR activity³² was determined at 37 °C in a mixture containing 0.25 mL of 1 mM glutathione disulfide, 0.25 mL of 0.36 mM NADPH, 0.25 mL of 4.5 mU/mL enzymatic solution, and 0.25 mL of 0.125 M sodium phosphate buffer (pH = 7.4) supplemented with 6.3 mM EDTA potassium salt, in a total volume of 1 mL.

2.4. Enzymatic Inhibition. The inhibitory activity of the newly synthesized compounds against ALR2, ALR1, SD, and GR was assayed adding 0.1 mL of the inhibitor solution to the reaction mixture described above. All the inhibitors were dissolved in water, and the solubility was facilitated by adjustment to a favorable pH. After complete dissolution, the pH was readjusted to 7. To correct for the nonenzymatic oxidation of NADPH or reduction of NAD⁺ and for absorption by the compounds tested, a reference blank containing all the above assay components except the substrate was prepared. The inhibitory effect of the new derivatives was routinely estimated at a concentration of 10^{-5} M. Those compounds

found to be active were tested at additional concentrations between 10^{-5} and 10^{-9} M. The determination of the IC₅₀ values was performed by using linear regression analysis of the log-dose–response curve, which was generated using at least four concentrations of inhibitors causing an inhibition between 20% and 80% with two replicates at each concentration. The 95% confidence limits (95% CL) were calculated from *t* values for $n - 2$, where *n* is the total number of determinations.

3. Pharmacology. 3.1. Materials and Methods. Experiments were carried out using Sprague Dawley albino rats, 45–55 g b.w., supplied by Harlan-Nossan Italy. Animal care and treatment conformed to the ARVO Resolution on the Use of Animals in Ophthalmic and Vision Research. The galactose diet consisted of a pulverized mixture of 50% D-galactose and 50% TRM (Harlan Teckland U.K.), laboratory chow, and the control diet consisted of normal TRM. Both control and experimental rats had access to food and water ad libitum.

3.2. Prevention of Cataract Development. Animals were randomly divided into groups of equal average body weight with 15 rats per group. The test compounds **55**, **59**, and tolrestat were administered four times daily as eyedrops of appropriate concentrations. The vehicle in which ARIs were contained was administered with the same dose regimen to the control group, which was given access to the galactose diet, and to the group fed with normal diet, which was included to record the aspect of normal lenses. Groups treated with the tested compounds were pre-dosed 1 day before switching their diet to galactose-containing chow. Lenses were examined using slit-lamp microscopy, after dilating the pupils with atropina 1% Farmigea, Italy, to establish their status of integrity.

Nuclear cataracts, which appeared as a pronounced central opacity readily visible as a white spot, were considered. The number of animals which attained this stage was recorded and the ability of the test compounds to prevent cataract development was assessed on the basis of comparison with galactosemic rats treated only with the vehicle.

4. Computational Procedures. Molecular modeling and other graphical manipulations were performed using the SYBYL 6.8⁴⁵ software package, running on a Silicon Graphics R10000 workstation. Model building of compound **55** was accomplished with the TRIPOS force field⁴⁶ available within SYBYL. Atomic point charges of this inhibitor were calculated with the semiempirical AM1⁴⁷ method implemented in the MOPAC program.⁴⁸ Energy minimizations and MD calculations were performed with the AMBER 4.1 program,^{49,50} using the all-atom Cornell et al. force field.⁵¹

4.1. Ligand Docking and MD Simulation. A starting model of compound **55** was obtained by modifying the crystal structure retrieved from a search by substructures using the October 2001 release of the Cambridge Structural Database (CSD)¹⁸ (refcode: LAYJIE). The carboxylate of the inhibitor was taken as dissociated. Atom-centered partial charges were calculated using the AM1 Hamiltonian⁴⁷ as implemented in MOPAC 6.0⁴⁸ (CHARGE = -1; keyword: MMOK). Geometry optimizations were achieved with the SYBYL/MAXIMIN2 minimizer by applying the BFGS (Broyden, Fletcher, Goldfarb and Shannon) algorithm⁵² and setting a root-mean-square gradient of the forces acting on each atom of 0.05 kcal/mol Å as gradient convergence criteria.

The pharmacophore-based conformations of *R*-**55** and *S*-**55**, obtained as described in Results and Discussion, were subjected to docking calculations into the ALR2 active site using the DOCK 3.5 suite of programs.^{36–39} Interestingly, the best scoring value for both enantiomers was achieved by the conformation yielding the best overlay on the TBI and the ALR2-bound conformation of zopolrestat. Docking of the *R*-**55** enantiomer generated 1054 orientations. Out of these, 83 were within 5 kcal/mol of the best orientation based on the scoring function (force field score of -35.9 kcal/mol). For the *S*-**55** enantiomer, out of the 1158 orientations generated by DOCK, the top-ranking 124 were within 5 kcal/mol from the best orientation based on the scoring function (force field score of -34.9 kcal/mol). Inspection of the docked structures revealed that the best and many of the top-scoring orientations of both

enantiomers placed the negatively charged carboxylate group of **55** in the anionic binding site of ALR2 lined by residues Tyr48, His110, and Trp111 so as to make a network of hydrogen bonds. From this cluster of structures, we selected the top-scoring orientation of the two enantiomers in which the *p*-tolyl ring was located in the same hydrophobic pocket occupied by the benzothiazole ring of zopolrestat in the crystal structure.

The parameters of the ligand were set consistently to the Cornell et al. force field: missing bond and angle parameters were assigned on the basis of analogy with known parameters in the database and calibrated to reproduce the AM1 optimized geometry. The complex was solvated by the addition of 217 TIP3P water molecules⁵³ within 20 Å of the inhibitor. After the protein, NADP⁺ and the inhibitor were frozen, and the water molecules alone were minimized (20 000 cycles or 0.1 kcal/mol rms deviation in energy) and equilibrated for 5 ps in a constant temperature (300 K) bath. SANDER energy minimization (<0.01 kcal/mol rms deviation) and 200 ps MD simulation of the entire system followed this. During dynamics, the positional constraints on the protein backbone were gradually reduced from 5 to 0.1 kcal/Å²/mol. The SHAKE was used to constrain bonds involving hydrogen. A 1-fs time step was used along with a nonbonded cutoff of 8 Å at 1 atm of constant pressure. The temperature was maintained at 300 K using Berendsen's algorithm⁵⁴ with a coupling constant of 0.2 ps. Four snapshots, extracted each 25 ps from the last 100 ps MD simulation, were found to be very similar in terms of rms deviation. An average structure was calculated from the last 100 ps trajectory and energy-minimized using the steepest descent and conjugate gradient methods available within the SANDER module of AMBER as specified above.

References

- Kador, P. F. The Role of Aldose Reductase in the Development of Diabetic Complications. *Med. Res. Rev.* **1988**, *8*, 325–352.
- Tomlison, D. R.; Stevens, E. J.; Diemel, L. T. Aldose Reductase Inhibitors and Their Potential for the Treatment of Diabetic Complications. *Trends Pharmacol. Sci.* **1994**, *15*, 293–297.
- Ammon, H. P. T.; Häring, H. U.; Kellerer, M.; Laube, H.; Mosthaf, L.; Verspohl, E. J.; Wahl, M. A. Antidiabetic Agents. Recent Advances in Their Molecular and Clinical Pharmacology. *Adv. Drug Res.* **1996**, *27*, 171–178.
- Ashizawa, N.; Tomoji, A. Benzothiazole Aldose Reductase Inhibitors. *Drugs Future* **1998**, *23*, 521–529.
- Costantino, L.; Rastelli, G.; Vianello, P.; Cignarella, G.; Barlocco, D. Diabetes Complications and Their Potential Prevention: Aldose Reductase Inhibition and Other Approaches. *Med. Res. Rev.* **1999**, *19*, 3–23.
- Sarges, R.; Oates, P. J. Aldose Reductase Inhibitors: Recent Developments. *Prog. Drug Res.* **1993**, *40*, 99–161.
- Da Settimo, F.; Primofiore, G.; Da Settimo, A.; La Motta, C.; Taliani, S.; Simorini, F.; Novellino, E.; Greco, G.; Lavecchia, A.; Boldrini, E. [1,2,4]Triazino[4,3-*a*]benzimidazole Acetic Acid Derivatives: A New Class of Selective Aldose Reductase Inhibitors. *J. Med. Chem.* **2001**, *44*, 4359–4369.
- Da Settimo, A.; Menicagli, C.; Nannipieri, E. Reactions of 2,3-Dibromoindole Derivatives with Bromine and Other Oxidizing Agents. 2,3-Dibromoindole → 3,3-Dibromooxindole Transformation. *J. Org. Chem.* **1974**, *39*, 1995–1998.
- Da Settimo, A.; Santerini, V.; Primofiore, G.; Biagi, G.; Veneziano, C. Bromination of Indole, Skatole and 2-Methylindole. Oxidation of 2-Bromoindole Derivatives. *Gazz. Chim. Ital.* **1977**, *107*, 367–372.
- Da Settimo, A.; Primofiore, G.; Ferrarini, P. L.; Franzone J. S.; Rocco, C.; Cravanzola, C. Bromoderivatives of Gramines. Preparation and Pharmacological Properties. *Eur. J. Med. Chem.* **1983**, *18*, 261–267.
- Primofiore, G.; Da Settimo, F.; Taliani, S.; Marini, A. M.; Novellino, E.; Greco, G.; Lavecchia, A.; Besnard, F.; Trincavelli, L.; Costa, B.; Martini, C. Novel N-(Arylalkyl)indol-3-ylglyoxylylamides Targeted as Ligands of the Benzodiazepine Receptor: Synthesis Biological Evaluation, and Molecular Modeling Analysis of the structure–Activity Relationships. *J. Med. Chem.* **2001**, *44*, 2286–2297.
- Howard, H. R.; Sarges, R.; Siegel, T. W.; Beyer, T. A. Synthesis and Aldose Reductase Inhibitory Activity of Substituted 2(1H)-Benzimidazolone- and Oxindole-1-acetic Acids. *Eur. J. Med. Chem.* **1992**, *27*, 779–789.
- Brittain, D. R.; Wood, R. Indoline Derivatives. *Eur. Pat. Appl.* EP 125,090; *Chem. Abstr.* **1985**, *102*, 113493f.
- Szabo-Pusztay, K.; Szabo, L. A Simple General Method for the Oxidation of Indoles to Oxindoles. *Synthesis* **1979**, 276–277.
- Wilson, D. K.; Tarle, I.; Petrash, J. M.; Quijcho, F. A. Refined 1.8 Å Structure of Human Aldose Reductase Complexed with the Potent Inhibitor Zopolrestat. *Proc. Natl. Acad. Sci. U.S.A.* **1993**, *90*, 9847–9851.
- Pietra, S. Indole Derivatives. *Farmaco* **1957**, *12*, 946–953.
- Harley-Mason, J.; Ingleby, R. F. J. Hydroxytryptamines. Part IV. Synthesis and Reactions of 2–3'-Oxindolyethylamines. *J. Chem. Soc.* **1958**, 3639–3642.
- Allen, F. H.; Bellard, S.; Brice, M. D.; Cartwright, B. A.; Doubleday, A.; Higgs, H.; Hummelink, T.; Hummelink-Peters, B. G.; Kennard, O.; Motherwell, W. D. S.; Rodgers, J. R.; Watson, D. G. The Cambridge Crystallographic Data Centre: Computer-Based Search, Retrieval, Analysis and Display of Information. *Acta Crystallogr.* **1979**, *B35*, 2331–2339.
- Morales-Rios, M. S.; Bucio-Vasquez, Ma. A.; Joseph-Nathan, P. Novel Oxidations of 1,3-Disubstituted Indoles. *J. Heterocycl. Chem.* **1993**, *30*, 953–956.
- Daisley, R. W.; Walker, J. Substituted Oxindoles. Pt VII. Oxindole Analogues of Tryptamine and its Derivatives. *Eur. J. Med. Chem.* **1979**, *14*, 47–52.
- Tacconi, G.; Righetti, P. P.; Desimoni, G. Preparation of N-Substituted Isatins. *J. Prakt. Chem.* **1973**, *315*, 339–344.
- De Ruiter, J.; Brubaker, A. N.; Garner, M. A.; Barksdale, J. M.; Mayfield, C. A. In Vitro Aldose Reductase Inhibitory Activity of Substituted N-benzenesulfonylglycine Derivatives. *J. Pharm. Sci.* **1987**, *76*, 149–152.
- Mayfield, C. A.; De Ruiter, J. Novel Inhibitors of Rat Lens Aldose Reductase: N-[(substituted amino)phenyl]sulfonylglycines. *J. Med. Chem.* **1987**, *30*, 1595–1598.
- Müller, P.; Hockwin, O.; Ohrloff, C. Comparison of Aldose Reductase Inhibitors by Determination of IC₅₀ with Bovine and Rat Lens Extracts. *Ophthalmic Res.* **1985**, *17*, 115–119.
- Hockwin, O.; Müller, P.; Krolczyk, J.; McCue, B. A.; Mayer, P. R. Determination of AL01576 Concentration in Rat Lenses and Plasma by Bioassay for Aldose Reductase Activity Measurements. *Ophthalmic Res.* **1989**, *21*, 285–291.
- Hu, T.; Merola, L. O.; Kuwabara, T.; Kinoshita, J. H. Prevention and Reversal of Galactose Cataract in Rats with Topical Sorbinil. *Invest. Ophthalmol. Vis. Sci.* **1984**, *25*, 603–605.
- Sestanjk, K.; Bellini, F.; Fung, S.; Abraham, N.; Treasurywala, A.; Humber, L.; Simard-Duquesne, N.; Dvornik, D. N-[5-(Trifluoromethyl)-6-methoxy-1-naphthalenyl]thioxomethyl-N-methylglycine (Tolrestat), a Potent, Orally Active Aldose Reductase Inhibitor. *J. Med. Chem.* **1984**, *27*, 255–256.
- Banditelli, S.; Boldrini, E.; Vilardo, G. P.; Cecconi, I.; Cappiello, M.; Dal Monte, M.; Marini, I.; Del Corso, A.; Mura, U. A New Approach Against Sugar Cataract Through Aldose Reductase Inhibitors. *Exp. Eye Res.* **1999**, *69*, 533–538.
- Chaudhry, P. S.; Cabrera, J.; Juliani, H. R.; Varma, S. D. Inhibition of Human Lens Aldose Reductase by Flavonoids, Sulindac and Indomethacin. *Biochem. Pharmacol.* **1983**, *32*, 1995–1998.
- Lindstad, R. I.; Hermansen, L. F.; McKinley-McKee, J. S. Inhibition and activation studies on sheep liver sorbitol dehydrogenase. *Eur. J. Biochem.* **1994**, *221*, 847–854.
- Ward, W. H. J.; Sennitt, C. M.; Ross, H.; Dingle, A.; Timmus, D.; Mirrless, D. J.; Tuffin, D. P. Ponalrestat, a Potent and Specific Inhibitor of Aldose Reductase. *Biochem. Pharmacol.* **1990**, *39*, 337–346.
- Fitzgerald, G. B.; Bauman, C.; Sajjat Hussoin, Md.; Wick, M. M. 2,4-dihydroxy benzylamine: a specific inhibitor of glutathione reductase. *Biochem. Pharmacol.* **1991**, *41*, 185–190.
- Camber, O.; Edman, P. Factors Influencing the Corneal Permeability of Prostaglandin F_{2α} and Its Isopropyl Ester in Vitro. *Int. J. Pharm.* **1987**, *37*, 27–32.
- Suhonen, P.; Järvinen, T.; Peura, P.; Urtti, A. Permeability of Pilocarpic Acid Diesters Across Albino Rabbit Cornea in Vitro. *Int. J. Pharm.* **1991**, *74*, 221–228.
- Chien, D.-S.; Tang-Liu, D. D.-S.; Woodward, D. F. Ocular Penetration and Bioconversion of Prostaglandin F_{2α} Prodrugs in Rabbit Cornea and Conjunctiva. *J. Pharm. Sci.* **1997**, *86*, 1180–1186.
- Meng, E. C.; Shoichet, B. K.; Kuntz, I. D. Automated Docking with Grid-Based Energy Evaluation. *J. Comput. Chem.* **1992**, *13*, 505–524.
- Meng, E. C.; Gschwend, D. A.; Blaney, J. M.; Kuntz, I. D. Orientational Sampling and Rigid-Body Minimization in Molecular Docking. *Proteins: Struct., Funct., Genet.* **1993**, *17*, 266–278.
- Shoichet, B. K.; Bodian, D. L.; Kuntz, I. D. Molecular Modeling Using Shape Descriptors. *J. Comput. Chem.* **1992**, *13*, 380–397.
- Connolly, M.; Gschwend, D. A.; Good, A. C.; Oshiro, C.; Kuntz, I. D. *DOCK 3.5*; Department of Pharmaceutical Chemistry, University of California: San Francisco, CA, 1995.
- Pietra, S.; Indole Derivatives. *Farmaco* **1958**, *13*, 75–79.

- (41) Arbuzov, A. E.; Bastanova, M. Sh. Tautomerism of Isatin. *Izvest. Akad. Nauk S. S. S. R., Otdel. Khim. Nauk* **1952**, 459–470; *Chem. Abstr.* **1953**, 47, 4876b.
- (42) Tacconi, G.; Gamba, A.; Marinone, F.; Desimoni, G. Heterodiene Syntheses-V. 1,2-Versus 1,4-Cycloaddition Reactions of Enamines to N-Substituted 3-Oxindolideneacetophenones. *Tetrahedron* **1971**, 27, 561–579.
- (43) Sadler, P. W. Synthesis of Antiviral Agents. Part I. Heterocyclic Compounds Related to Isatin 3-Thiosemicarbazone. *J. Chem. Soc.* **1961**, 243–246.
- (44) Hayman, S.; Kinoshita, J. H. Isolation and Properties of Lens Aldose Reductase. *J. Biol. Chem.* **1965**, 240, 877–882.
- (45) *Sybyl Molecular Modelling System (version 6.8)*; Tripos: St. Louis, MO.
- (46) Vinter, J. G.; Davis, A.; Saunders, M. R. Strategic Approaches to Drug Design. 1. An Integrated Software Framework for Molecular Modelling. *J. Comput.-Aided Mol. Des.* **1987**, 1, 31–55.
- (47) Dewar, M. J. S.; Zoebisch, E. G.; Healy, E. F.; Stewart, J. J. P. AM1: a New General Purpose Mechanical Molecular Model. *J. Am. Chem. Soc.* **1985**, 107, 3902–3909.
- (48) MOPAC (version 6.0) is available from Quantum Chemistry Program Exchange, No. 455.
- (49) Pearlman, D. A.; Case, D. A.; Caldwell, J. W.; Ross, W. S.; Cheatham, T. E., III.; Debolt, S.; Ferguson, D. M.; Seibel, G. L.; Kollman, P. A. AMBER, a Package of Computer Programs for Applying Molecular Mechanics, Normal-Mode Analysis, Molecular Dynamics and Free Energy Calculations to Simulate the Structural and Energetic Properties of Molecules. *Comput. Phys. Commun.* **1995**, 91, 1–41.
- (50) Pearlman, D. A.; Case, D. A.; Caldwell, J. W.; Ross, W. S.; Cheatham, T. E., III; Ferguson, D. M.; Seibel, G.; Singh, U. C.; Weiner, P. K.; Kollman, P. A. *AMBER 4.1*; Department of Pharmaceutical Chemistry, University of California: San Francisco, CA, 1995.
- (51) Cornell, W. D.; Cieplak, P.; Bayly, C. I.; Gould, I. R.; Merz, K. M.; Ferguson, D. M.; Spellmeyer, D. C.; Fox, T.; Caldwell, J. W.; Kollman, P. A. A Second Generation Force Field for the Simulation of Proteins, Nucleic Acids, and Organic Molecules. *J. Am. Chem. Soc.* **1995**, 117, 5179–5197.
- (52) Head, J.; Zerner, M. C. A Broyden-Fletcher-Goldfarb-Shanno Optimization Procedure for Molecular Geometries. *Chem. Phys. Lett.* **1985**, 122, 264–274.
- (53) Jorgensen, W. L.; Chandrasekhar, J.; Madura, J. D.; Impey, R.; W.; Klein, M. L. Comparison of Simple Potential Functions for Simulating Liquid Water. *J. Chem. Phys.* **1983**, 79, 926–935.
- (54) Berendsen, H. J. C.; Postma, J. P. M.; van Gunsteren, W. F.; DiNola, A.; Haak, J. R. Molecular Dynamics with Coupling to an External Bath. *J. Chem. Phys.* **1984**, 81, 3684–3690.

JM030762F